Physics and Chemistry of Minerals (2019) 46:37–49
https://doi.org/10.1007/s00269-018-0985-7

ORIGINAL PAPER

Systematic theoretical study of [001] symmetric tilt grain boundaries in MgO from 0 to 120 GPa

Pierre Hirel[1] · Gabriel Franck Bouobda Moladje[1] · Philippe Carrez[1] · Patrick Cordier[1]

Received: 13 November 2017 / Accepted: 30 June 2018 / Published online: 4 July 2018

Abstract
The properties of [001] symmetric tilt grain boundaries (STGBs) in magnesium oxide are investigated systematically with atomic-scale simulations. Their formation energies, atomic structures, and excess volumes are computed. STGBs are found to prefer a symmetric configuration, except for tilt angles larger than 67.4°, where the decomposition of the STGBs into ½[110] dislocations is preferred. Then, the effects of pressure are investigated from 30 up to 120 GPa, a pressure range relevant to the Earth's lower mantle. Pressure is found to change the atomic configuration of all investigated GBs, sometimes several times as pressure increases. We also find that these changes are irreversible, the GBs retaining their high-pressure configuration even after pressure is released. Implications for the deformation of ferropericlase in the conditions of the Earth's lower mantle are discussed.

Keywords Computer simulation · Magnesium oxide · Grain boundaries

Introduction

Magnesium oxide (MgO) is a ceramic compound known for its ductility, enhanced by the high mobility of dislocations (Tromas et al. 1999). In the interior of the Earth, iron-bearing MgO (i.e., ferropericlase) is considered to be the second most abundant phase of the Earth's lower mantle (Ringwood 1991). Many studies have strengthened our understanding of intra-crystalline plasticity of MgO (Appel et al. 1977; Tromas et al. 1999; Amodeo et al. 2011). In polycrystalline aggregates, the properties of grain boundaries (GBs) are critical to the understanding of the mechanical behaviour. In the laboratory, deformation of aggregates of bridgmanite and ferropericlase has shown that the former, which is the weaker, localises the strain leading to grain elongation and fragmentation (Girard et al. 2015; Nzogang 2018), i.e., in an increase of the GB fraction. In a high-temperature regime, GBs are expected to play a key role in grain growth, in strain production by GB migration (Sun et al. 2017), or in controlling point defects' concentrations by acting as sources or sinks for vacancies (Karki et al. 2015). Being a source of excess volume, GBs are also good candidates for the segregation of incompatible elements such as heat-producing elements or rare gases (Hiraga et al. 2004; Karki et al. 2015).

In a series of papers, Harris et al. investigated the properties of grain boundaries in MgO using atomic-scale simulations (Harris et al. 1996, 1997, 1999; Watson et al. 1996). Their work included explicitly the effect of pressure and temperature, and they showed that GBs change their atomic configuration with increasing pressure and that this change was irreversible, i.e., the GBs retain their high-pressure configuration even when brought back to ambient pressure. However, due to computational limitations at the time, they restricted their study to a very small number of GBs, namely, the [001] symmetric tilt GBs with $\{n10\}$ contact surfaces, with n ranging from 1 to 5. Whether their conclusions are applicable to other types of grain boundaries remains to be determined.

More recently, ab initio calculations have provided valuable information about the atomic and electronic structures of GBs (McKenna and Shluger 2009; Verma and Karki 2010), confirming with very accurate first-principles methods that the atomic structure of GBs is indeed sensitive to pressure. However, despite the accuracy of such methods, different formation energies were reported for the same {310}[001] tilt grain boundary: 1.95 J m^{-2} from McKenna and Shluger

✉ Pierre Hirel
pierre.hirel@univ-lille1.fr

[1] University of Lille, CNRS, INRA, ENSCL, UMR 8207 UMET-Unité Matériaux et Transformations, 59000 Lille, France

(2009), versus 1.51 J m^{-2} from Verma and Karki (2010). Such a discrepancy may be attributed to the limited system size, the use of different DFT functionals, and to different corrections applied, each contributing to the uncertainty of the calculation. Finally, owing to their high computational cost, those ab initio calculations were again restricted to a very small number of low-index GBs. Such methods are not well suited to perform a systematic study, and obtain general and statistical information about GBs.

In this work, we use atomistic simulations to perform a systematic study of the properties of [001] symmetric tilt grain boundaries (STGBs) in MgO. The computational efficiency of this method allows to investigate over 200 GBs and to obtain relevant data about their structure and formation energies. The pressure is varied from 0 GPa, relevant to MgO as a ceramic material, up to 120 GPa, corresponding to the conditions at the bottom of the Earth's lower mantle. The study focuses more on understanding the global behaviour of this type of GBs using statistical analysis than on detailed properties of individual GBs.

Methods and models

Potential model

Chemical bonding in MgO is mainly ionic, and can be described with a rigid-ion pair potential function, composed of the Coulomb interaction and a short-range Buckingham potential:

$$U_{ij} = \frac{q_i q_j}{R_{ij}} + b_{ij} \exp\left(\frac{-R_{ij}}{\rho_{ij}}\right) - \frac{c_{ij}}{R_{ij}^6}. \quad (1)$$

The Coulomb potential is evaluated at short range in real space, and at long range in reciprocal space, by means of the particle–particle–particle–mesh (pppm) method (Eastwood et al. 1980; Hockney and Eastwood 1988). The ion charges q_i and the terms b_{ij}, ρ_{ij}, and c_{ij} are adjustable parameters. We use the parameterization of Henkelman et al. (2005), which was initially fitted to describe the migration of MgO dimers on MgO surfaces. It was shown that this potential describes accurately the equation of state of MgO, the energy of stacking faults, as well as the dislocation core structures, for pressures ranging from 0 to 100 GPa (Carrez et al. 2015). The ability of this potential to describe complex defects in such a wide range of conditions makes it an ideal candidate to model grain boundaries.

Construction of grain boundaries

The grain boundaries (GBs) investigated are symmetric tilt grain boundaries (STGBs), noted $\{hk0\}[001]$, where grains are rotated by opposite angles around the same [001] axis. The choice of the [001] tilt axis is manifold. First, along this axis, each atomic column contains an equal number of magnesium and oxygen ions, which ensures that all the tilt grain boundaries constructed are charge neutral. Second, this type of grain boundaries has been observed with high-resolution microscopy (Saito et al. 2013; Bean et al. 2017), as well as modelled using ab initio (McKenna and Shluger 2009; Verma and Karki 2010) or force-field simulations (Watson et al. 1996; Harris et al. 1999; Yokoi and Yoshiya 2017), providing data to compare our results to.

The systems containing grain boundaries are constructed with Atomsk (Hirel 2015). Two crystals of MgO are rotated by opposite angles $\pm\alpha/2$, cut and then stacked together, thus forming an STGB. The surface S of the GB depends on the misorientation angle α between the two crystals. Boundary conditions are 3D periodic, so that there are actually two GBs in the simulation cell. The dimensions of the cell are carefully chosen, so that the two GBs are equivalent, and contribute equally to the total energy. The formation energy of the GB is then defined as

$$E_{\mathrm{GB}}(\alpha) = \left(E_1(\alpha) - E_0\right)/2S, \quad (2)$$

where $E_1(\alpha)$ is the total energy of the system containing the GBs, E_0 is the total energy of a supercell of perfect (defect-free) crystal containing the same number of atoms, and $2S$ is the total surface of the two GBs that exist in the cell. The computed formation energy is sensitive to the system size, i.e., to the distance between periodic replicas of GBs. By computing the formation energy of $\{210\}[001]$, $\{310\}[001]$, and $\{410\}[001]$ GBs for various system sizes, we find that a minimum distance of 60 Å between two consecutive GBs is necessary to obtain a good convergence of the energy. To ensure that all GB energies are converged, in the following we construct all systems with GB distances d_{GB} greater than 100 Å (i.e., the supercell dimension perpendicular to the GB is greater than 200 Å).

After construction, the total energy of the system is minimized by means of a conjugate-gradient algorithm. A pitfall of such an algorithm is that it converges towards the closest minimum of energy, which may not be the global minimum of energy. To circumvent this limitation, we follow a scheme similar to the one used by Harris et al. (1996), and commonly used when performing atomic-scale simulations of GBs. The top grain is shifted along the GB plane by a vector $\boldsymbol{\tau}$, and atoms are allowed to relax in the direction normal to the GB, thus providing the energy landscape as a function of the shift vector $\boldsymbol{\tau}$, also called γ-surface. Among those configurations, the one of the lowest energy is selected, and atoms are allowed to relax in all directions, yielding the absolute minimum energy of the GB.

Finally, we design an algorithm to construct and relax all GBs. For a given tilt angle α, the system containing a GB

is constructed with the constraint that the distance between GBs is at least 100 Å to ensure good convergence. To keep the simulation times reasonable, atomic systems containing more than 100,000 ions are excluded. Otherwise, a full γ-surface calculation is performed as explained above, yielding the final formation energy of this grain boundary. The procedure is repeated for all tilt angles α from 0° to 90° by increments of 0.1°, thus providing the minimum formation energy as a function of the tilt angle, $E_{GB}(\alpha)$.

Results at ambient pressure

GB formation energies

The procedure described above allowed us to construct systematically over 200 STGBs, find their optimal atomic configuration, and compute their minimum formation energies.

The formation energies of [001] STGBs are represented in Fig. 1, as a function of the misorientation α between the two grains. The angle $\alpha = 0°$ corresponds to a perfect crystal without a grain boundary, and is taken as reference of the energies. From 0° to about 20° (referred to as low-angle STGBs), the energy gradually increases, reaching about 1.7 J m^{-2} for an angle of 20°.

In the range $20° < \alpha < 67.4°$, most grain boundaries have similar energy values of about 1.7 J m^{-2}. Noticeable exceptions are the {310}[001] grain boundary ($\alpha = 36.8°$), the energy of which is slightly smaller than average, and the

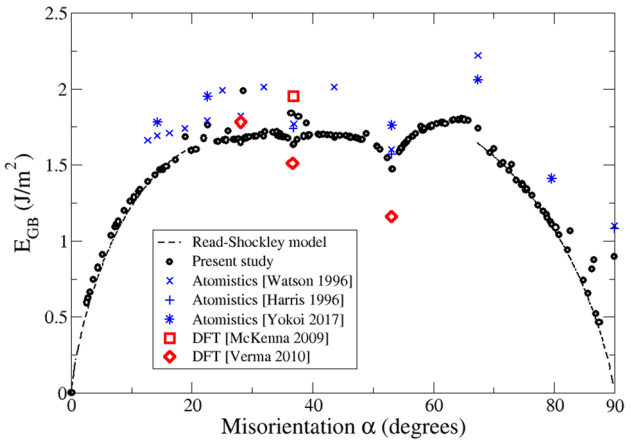

Fig. 1 Computed energy of formation of [001] symmetric tilt grain boundaries in MgO at 0 GPa, as a function of the misorientation α between the two crystals. The results of the present study (black circles) are compared with the previous atomistic calculations by Watson et al. (1996) (blue crosses), Harris et al. (1996) (blue plus signs), and Yokoi and Yoshiya (2017) (blue stars); and with ab initio results from McKenna and Shluger 2009 (red square) and from Verma and Karki (2010) (red diamonds). The bulk system containing no defect ($\alpha = 0$) serves as a reference of the energy. The results of the analytical Read–Shockley model (Eq. 3) are also shown (dashed lines)

{210}[001] GB ($\alpha = 53.1°$) which has an energy of about 1.47 J m^{-2}, significantly lower than other high-angle GBs, forming a significant dip in the energy curve. The particularly low formation energies of these two GBs indicate that they are somewhat special; hence, their properties may not be representative of all STGBs.

The GB corresponding to a tilt angle equal to 67.4° marks a discontinuity in terms of formation energies. For tilt angles larger than 67.4°, the energy of STGBs decreases, vanishing as the misorientation approaches 90°. The reason for this discontinuity and the atomic structure of those peculiar GBs are detailed later.

Finally, when the misorientation between the two crystals is exactly equal to $\alpha = 90°$, the configuration is equivalent to the [−110](110) stacking fault. For this particular configuration, no γ-surface calculation was performed, because shifting one crystal with respect to the other results in the formation of a bulk, defect-free MgO single crystal, which of course has no excess energy compared to the reference $\alpha = 0°$. We find that the [−110](110) stacking fault is metastable, with a formation energy $E_{SF} = 0.898$ J m^{-2}. This value is somewhat lower than the one obtain by Harris et al. (1996) with a different atomistic potential ($E_{SF} = 1.08$ J m^{-2}), and also lower than the one obtained by Carrez et al. (2009) using ab initio methods ($E_{SF} = 1.05$ J m^{-2}), but remains within a 15% error margin.

Atomic structure

As explained in the methods, the optimal STGB configurations were found by shifting the top grain with respect to the bottom grain by a vector $\boldsymbol{\tau}$. In the as-constructed configurations ($\boldsymbol{\tau} = 0$), ions of different species face each other across the boundary, forming Mg–O bonds. When the top crystal is shifted ($\boldsymbol{\tau} \neq 0$), then atoms of the same species may face across the boundary, forming Mg–Mg and O–O bonds.

For tilt angles α close to zero, all investigated STGBs remain symmetric at 0 GPa. They relax by forming an array of geometrically necessary dislocations (GNDs) of edge character, with a Burgers vector $\boldsymbol{b} = [010]$, and spread in (100) planes, as shown by the example of the low-angle (5.4°) GB in Fig. 2a. These [010] dislocations are characterized by a very open core. This type of STGB corresponds to the Read–Shockley model (Read and Shockley 1950) that describes them as an array of dislocations separated by a distance d, yielding a GB energy:

$$E_{RS} = \frac{\mu b^2}{4\pi d(1-\nu)}\,[A - \ln(\alpha)], \tag{3}$$

where $\mu = 138.1$ GPa is the material's shear modulus, $\nu = 0.33$ is its Poisson ratio, b is the magnitude of the Burgers vector of the dislocations, and $A = 1 + \ln(b/2\pi r_0)$ with r_0

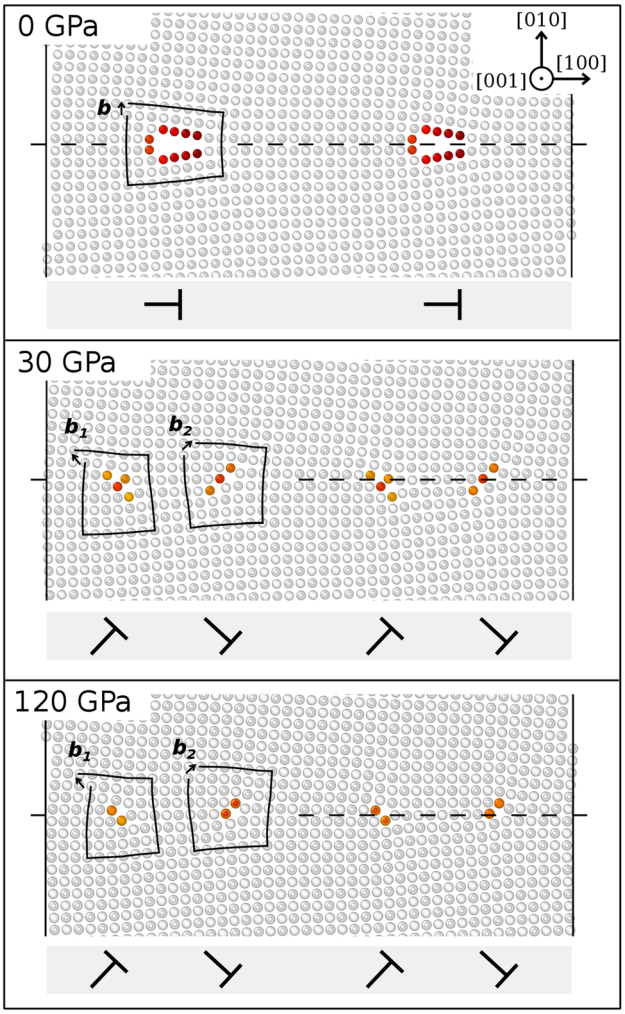

Fig. 2 Evolution with pressure of the optimal atomic configuration of a low-angle ($\alpha = 5.2°$) tilt GB. Atoms in near-perfect environment are displayed in light grey, those in defects appear in colour, according to their central symmetry parameter (Kelchner et al. 1998). The [001] direction is normal to the figure, and the GB plane, indicated by the horizontal dashed line, is normal to the [010] direction. Burgers circuits are drawn around some dislocations. At 0 GPa, the closing Burgers vector is $\boldsymbol{b}$ = [010]; at 30 GPa and above, it decomposes into two dislocations of Burgers vectors $\boldsymbol{b}_1$ = ½[−110] and $\boldsymbol{b}_2$ = ½[110]. Visualization performed with OVITO (Stukowski 2010)

is the radius of the dislocation core. This analytical function is plotted in Fig. 1 for low-angle GBs (dashed line from $\alpha = 0°$ to 20°), using a Burgers vector $\boldsymbol{b}$ = [010], and fitting to the results of atomistic simulations yields a value $r_0 = 0.65b$ for the dislocation core radius.

High-angle grain boundaries ($20° < \alpha < 67.4°$) cannot be described solely in terms of dislocation density, and hence do not respond to the Read–Shockley model. Figure 3 shows some examples of high-angle GBs. Most of them are composed of structural units, with patterns that depend on the tilt angle, and that contain a wide opening or void. Yet, most of the high-angle GBs remain symmetric ($\boldsymbol{\tau} = 0$). Another remarkable feature is that at ambient pressure, no atom inhabits the plane of the boundary: atoms remain above or below the GB, inside their respective crystal, forming Mg–O bonds across the boundary. These features are found in most high-angle GBs, up to the tilt angle $\alpha = 67.4°$ which corresponds to a particular configuration, that is the {320} [001] STGB.

As stated earlier, the misorientation of 67.4° marks a discontinuity in the energy curve. Above this tilt angle, most GBs have a lower energy if the top crystal is shifted with respect to the bottom one, by a vector $\boldsymbol{\tau}$= ½[001]. This is strikingly different from the previous low- and high-angle GBs. We find that if no shift is allowed, those GBs relax by forming regular structural units, similar to the ones observed in high-angle GBs. On the contrary, when allowing the top crystal to move along the GB plane, the GBs decompose into individual ½[110] dislocations separated by perfect crystal, as shown in Fig. 4. It must be related to the fact that, if a shift $\boldsymbol{\tau}$= ½[001] is allowed for the configuration $\alpha = 90°$, the GB disappears completely and leaves only a defect-free single crystal, as explained in the previous section. By analogy, when the misorientation is slightly smaller than 90°, it is most favourable to shift a crystal with respect to the other by a vector $\boldsymbol{\tau}$ = ½[001] to recover as much perfect crystal as possible, which minimizes the energy, and the misorientation being accommodated by GNDs. Since the crystals were rotated by angles close to ±45°, those GNDs spread into (1–10) planes, which are almost normal to the GB plane. This decomposition into individual dislocations significantly decreases the GB energies. We plotted the Read–Shockley Eq. (3), using this time a Burgers vector $\boldsymbol{b}$ = ½[110], for angles between 67.4° and 90°, as shown in Fig. 1. This time, fitting to atomistic results, yields $r_0 = 0.4b$. It is inferred that this shift is necessary for the GNDs to form when the misorientation between the two crystals lies between 67.4° and 90°.

Excess volumes

The formation of a grain boundary causes an expansion of the crystal, quantified by the excess volume due to GNDs or to the structural units. The excess volume V_{GB} of a grain boundary is defined as the difference between the volume V_1 of the cell containing the GB and the volume V_0 of a perfect crystal containing the same number of atoms, normalized to the total area of the two GBs in the simulation cell:

$$V_{GB}(\alpha) = \left(V_1(\alpha) - V_0\right)/2S. \tag{4}$$

Excess volumes for STGBs at ambient pressure are reported in Fig. 5 as open circles. Low-angle grain boundaries (i.e., when α is close to 0° or 90°) have low excess volumes, while high-angle grain boundaries tend to have larger excess volumes, up to about 1.2 $Å^3/Å^2$. These values

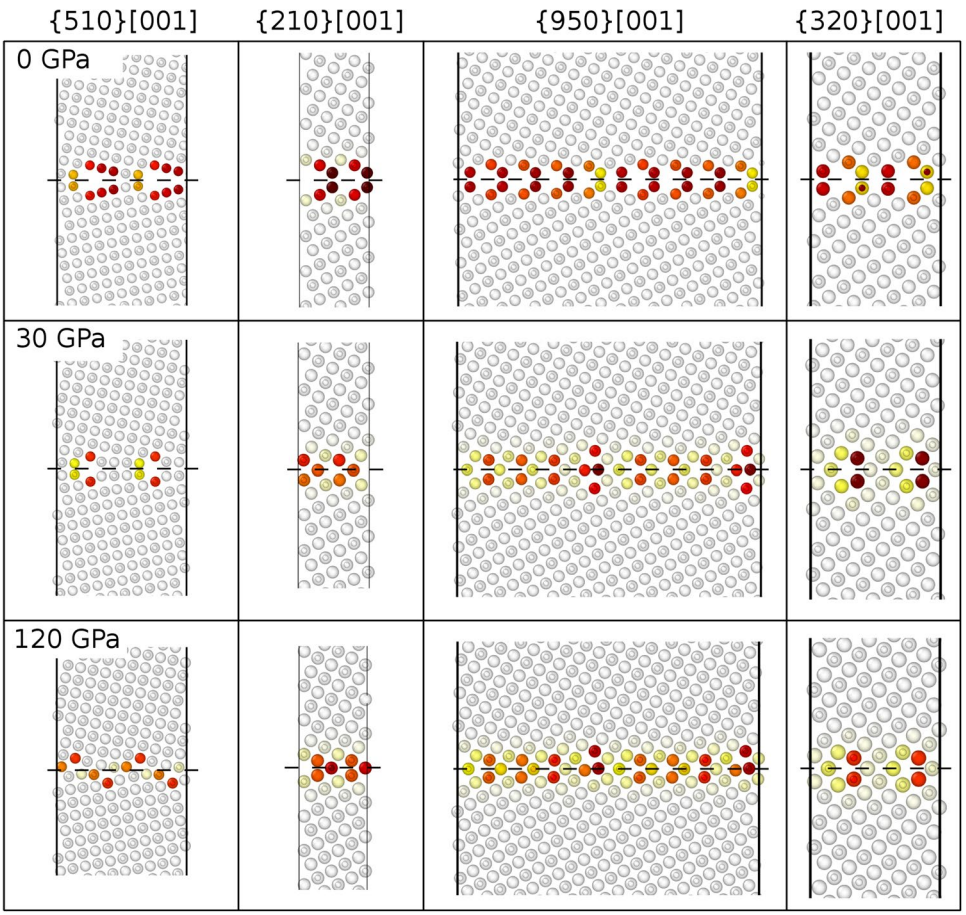

Fig. 3 Evolution with pressure of the optimal atomic configuration of some high-angle GBs (same colour convention, as shown in Fig. 2). The grain boundaries are: {510}[001] ($\alpha = 22.6°$);{210}[001] ($\alpha = 53.1°$); {950}[001] ($\alpha = 58.1°$); {320}[001] ($\alpha = 67.4°$)

are in good agreement with the ones obtained by Yokoi and Yoshiya (2017) (represented as blue stars in Fig. 5), indicating that the excess volume may be less sensitive to the interatomic potential than the formation energies.

The relationship between formation energies and excess volumes is reported in the inset graph of Fig. 5. There is a strong tendency for high-excess volume GBs to also have high formation energies, which correspond to misorientations α ranging from about 20° to 50°. However, GBs that have a low excess volume can have either a low formation energy (misorientations $0° < \alpha < 20°$ and $70° < \alpha < 90°$), or have high formation energies ($50° < \alpha < 70°$). As a result, no continuous relationship between excess volumes and formation energies can be extracted from the data.

Effects of pressure

Formation energy

Now, we investigate the effect of pressure on the energy and atomic structure of grain boundaries. Knowing the equation of state of MgO, pressure is applied by an appropriate rescaling of the simulation cell, followed by an optimization of the cell size based on atomic forces to reach the target pressure. Then, a new γ-surface calculation is performed to obtain the optimal atomic configuration of the GB at this pressure. Pressure is increased by steps of 30 GPa up to 120 GPa, i.e., in a range relevant to the Earth's lower mantle. At high pressure (and not accounting for the effects of temperature), the relevant quantity to compare is the system's enthalpy; therefore, we will discuss the formation enthalpy of STGBs.

The enthalpy of formation of STGBs is reported as a function of the misorientation, as shown in Fig. 6. The previous data at ambient pressure appear as black dots. Increasing the pressure to 30 GPa (green triangles) increases significantly the formation enthalpy of all GBs. Contrary to ambient pressure, where most STGBs had very similar energies, at 30 GPa, there is a wide dispersion of energies, with values ranging from 2 up to 3.1 J m^{-2} for high-angle STGBs. We will see later that this dispersion is related to changes in the atomic structures of GBs.

At 60 GPa (blue crosses), STGB formation enthalpies increase further, with a less marked dispersion. For high-angle GBs, it averages to about 4.2 J m^{-2}. Finally, increasing the pressure up to 90 GPa (open squares) and 120 GPa (filled

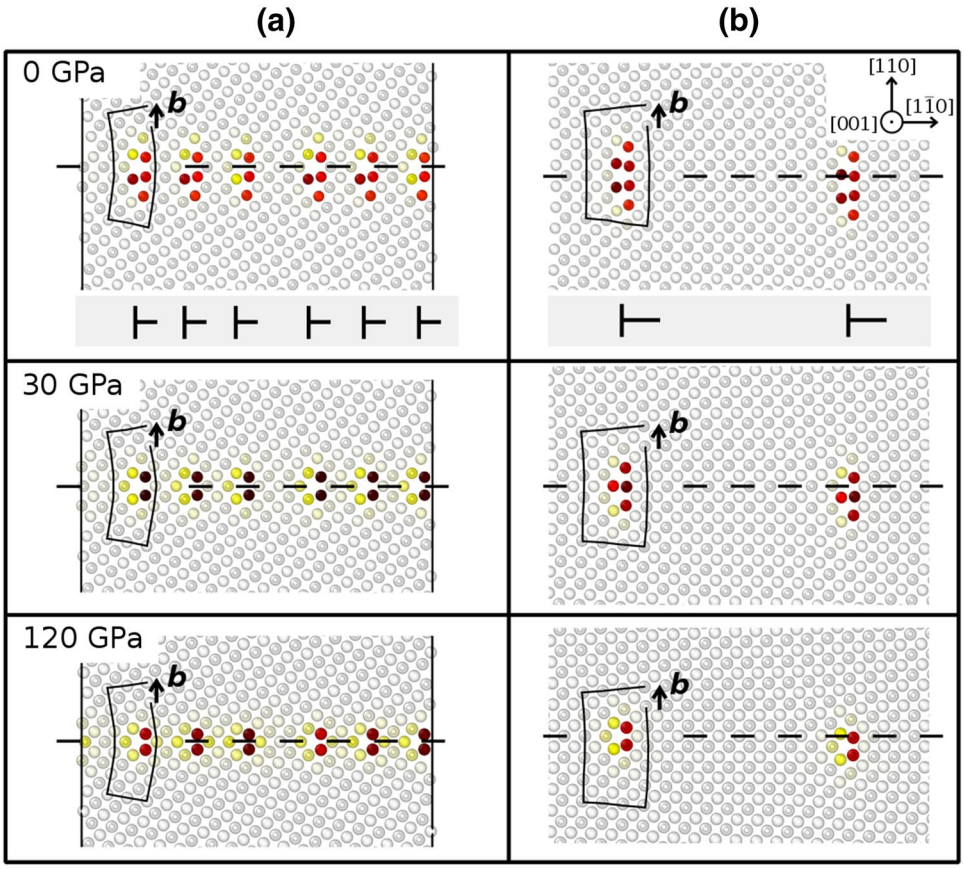

Fig. 4 Evolution with pressure of the atomic configuration of near-right angle STGBs. The misorientations between the two crystals are: **a** $\alpha = 70°$; **b** $\alpha = 84.8°$. Those GBs decompose into an array of ½[110] (1–10) edge dislocations, as schematized by the $\perp$ signs (same colour conventions, as shown in Fig. 2). The crystal directions are given for GBs in column **b**, where the GB plane is almost normal to the [110] direction. Note that since each crystal was rotated by an angle close to 45°, the crystal directions are different from Fig. 2

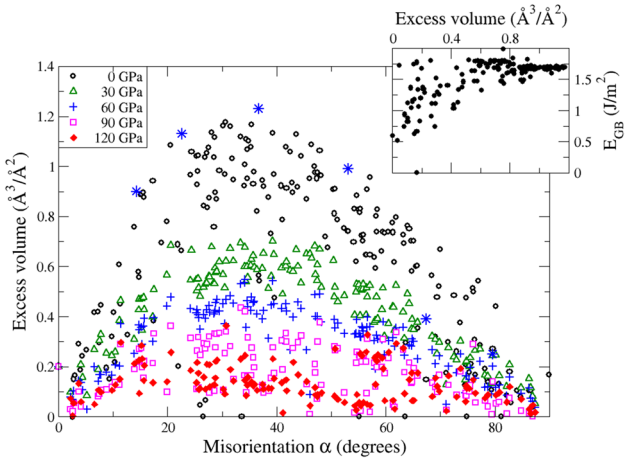

Fig. 5 Evolution of GB excess volumes with pressure. Excess volume is reported versus the misorientation for ambient pressure (open circles), and pressures equal to 30 GPa (open triangles), 60 GPa (crosses), 90 GPa (open squares), and 120 GPa (filled diamonds). The blue stars are the data at ambient pressure from Yokoi and Yoshiya (2017). The inset graph shows the relationship between formation energies and excess volumes at 0 GPa, for all GB studied

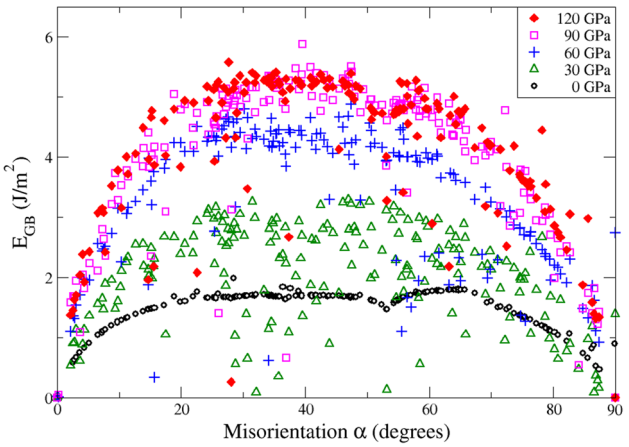

Fig. 6 Evolution with pressure of the enthalpy of formation of grain boundaries as a function of the tilt angle at 0 GPa (open circles, same as Fig. 1), 30 GPa (open triangles), 60 GPa (crosses), 90 GPa (open squares), and 120 GPa (filled diamonds)

diamonds) leads to a saturation of the formation enthalpy, reaching about 5.2 J m^{-2}.

Atomic structure

The observation of STGBs at high pressure reveals that most of them undergo a drastic modification of their atomic structure, with respect to the ones that they have at ambient pressure. At 30 GPa, most GBs favour a more compact configuration, where the patterns with large vacant sites typical to ambient pressure are replaced with more compact structural units. To reach these new configurations, in many cases, the top crystal has to be shifted with respect to the bottom one, so that $\boldsymbol{\tau} \neq (0,0)$. While at ambient pressure, the ions preserved their local environment, at high-pressure atoms of the same chemical species face each other across the GBs, forming Mg–Mg and O–O bonds. Contrary to ambient pressure, atoms do not remain on their respective side of the boundary: in many cases, atoms are found within the plane of the boundary.

Low-angle STGBs, that are described by [010](100) GNDs at ambient pressure, decompose at high pressure into arrays of ½<110> dislocations and spread into {110} planes that form an angle about 45° with the GB plane, as shown in Fig. 2. This is strikingly different from ambient pressure, where [010] GNDs were energetically more favourable.

High-angle STGBs ($20° < \alpha < 67.4°$), which cannot be described solely in terms of GNDs, do not know such a transition. Yet, their structural units do undergo significant modifications. Atoms tend to occupy the large vacant sites that existed at ambient pressure, closing the gaps to achieve greater compaction. The closing of GB structural units may happen in several steps as pressure increases, and some GBs have different atomic structure at 30 and at 120 GPa, as shown in Fig. 3. This is consistent with the recent work of Yokoi and Yoshiya (2017), who found several transformations of STGB atomic structure when pressure increases. We conclude that the effect of pressure on STGBs is not continuous, but discontinuous throughout the mantle. As a result, it is sensible to expect their properties (like their energy or mobility) to change in a non-linear way.

When pressure increases, in most cases, the STGBs prefer a configuration where one grain is shifted with respect to the bottom grain by a vector $\boldsymbol{\tau}$ contained in the GB plane. At 0 GPa, most STGBs prefer the as-constructed configuration $\boldsymbol{\tau} = (0,0)$, as explained earlier. This is not true anymore when pressure increases. At 30 GPa, the initial configuration $\boldsymbol{\tau} = (0,0)$ is the most favourable for only 26.8% of the STGBs investigated, meaning that about 73.2% become asymmetric at high pressure. At 120 GPa, about 86.6% of the STGBs are asymmetric. These statistics show that there is a general tendency for STGBs to shift from a symmetric configuration at ambient pressure, towards an asymmetric one at high pressure.

Excess volumes

Figure 5 shows the evolution of STGB excess volumes with pressure. As expected from the application of pressure and the changes in atomic structures, the excess volumes decrease drastically as pressure increases. The largest drop happens when bringing GBs from ambient pressure up to 30 GPa, which decreases the maximum excess volumes from about 1.2 $Å^3/Å^2$ down to 0.7 $Å^3/Å^2$ (− 42%). Further increasing the pressure continues to decrease excess volumes, which become as low as 0.3 $Å^3/Å^2$ at 120 GPa (− 75% with respect to values at 0 GPa).

Irreversibility of structure change

An interesting result of the work of Harris et al. (1996) and Yokoi and Yoshiya (2017) is that, after pressure has been applied and an STGB has adopted a more compact atomic configuration, it retains this structure even when pressure is released. In other words, STGBs keep a memory of the compaction inherited from high pressure.

We wanted to verify if this conclusion holds for all the STGBs that we studied. Starting from the configurations obtained at 30 GPa, we decreased the pressure to 0 GPa and performed an atomic relaxation. This time, no γ-surface calculation is performed, since it would yield the absolute minimum of energy, which was already found previously. The purpose here is to test if the high-pressure atomic configurations remain metastable at ambient pressure.

Indeed, we find that most STGBs do not relax back to their absolute minimum of energy, but keep their high-pressure configuration. It means that these configurations, although not the most favourable ones, are at least metastable at ambient pressure.

As an example, the {520}[001] STGB changes from an array of [010] dislocations at ambient pressure, into an array of ½<110> dislocations at 30 GPa (Fig. 3). When the latter is relaxed back to ambient pressure, the ½<110> dislocation array remains, showing that it is a metastable configuration of the GB. The total energy of the system is, however, larger than that of the initial GB containing [010] dislocations. Indeed, our simulations indicate that the array of [010] GNDs is the most favourable configuration at ambient pressure and in the absence of any stress. Yet, this slip system is not at all favourable. It is likely that, under applied stress of any kind (whether it is isostatic pressure like here, or uniaxial or shear stress), those [010] dislocations tend to decompose into ½<110> dislocations, which belong to the most favourable slip systems. For the same reason, low-angle GBs that form during a recovery process are much more likely to involve ½<110> dislocations, which are glissile, rather than [010] dislocations, which do not nucleate or multiply easily when the material is deformed. Therefore,

although our simulations predict [010] GNDs to be stable inside low-angle STGBs, they are unlikely to be observed in experimentally prepared or natural samples.

Similarly, the high-angle STGBs studied keep their compact high-pressure configuration when pressure is released. As an example, the {210}[001] STGB has a compact atomic structure at 30 GPa (Fig. 3), which remains metastable when pressure is removed. This is again consistent with the work of Yokoi and Yoshiya (2017), who also concluded that the compact configurations that are stable at high pressure remain metastable when pressure is released. Hence, MgO polycrystals sintered under high pressure are expected to contain more compact, less mobile GBs, than those synthesized at ambient pressure.

In natural rock samples containing ferropericlase, originating either from the Earth's interior or from other celestial bodies, the irreversibility of STGB atomic configuration may be used to determine their pressure history. Observation of the detailed atomic structure of GBs in natural samples, or even just their compaction or excess volume, may be used as a proxy to determine their conditions of formation and/or evolution.

Discussion

Reliability

Overall, the energy values derived from our classical force-field simulations compare qualitatively well with the ones from the previous atomistic calculations (Harris et al. 1996; Watson et al. 1996; Yokoi and Yoshiya 2017). The quantitative discrepancies can be attributed to the use of different interatomic potentials, leading to different absolute values of the formation energies.

Comparison with ab initio calculations is more difficult, because data available from the literature are scarce and not always consistent. For instance, two very different values were reported for the formation energy of the {310}[001] STGB ($\alpha = 36.8°$): 1.95 J m^{-2} by McKenna and Shluger (2009) and 1.51 J m^{-2} by Verma and Karki (2010). Our value of 1.63 J m^{-2} falls between those two, although it is closer to the latter value of Verma and Karki. Furthermore, our calculations indicate that some GBs are special, like the {210}[001] that corresponds to a significant drop in the energy curve (Fig. 1). Unfortunately, ab initio studies so far have focused on those special cases, owing to computational limitations. As a result, it is challenging to derive the global behaviour of STGBs from the available ab initio data, for comparison with the present study. It would be valuable to obtain further results from ab initio calculations, concerning higher index GBs, to further validate the present conclusions.

Yet, force-field simulations also have their limitations. For instance, a well-known pitfall of the pair potential of Henkelmann used in the present study is that it does not reproduce the violation of the Cauchy relationship in MgO (Carrez et al. 2009). Because of the limited accuracy of our model, the absolute values presented above should be considered with care. We obtain a good qualitative agreement with other force-field simulations, and even with ab initio results, to some extent. Yet, the most interesting conclusions of the present study lie in the global behaviour of GBs and their evolution with pressure. For instance, the average STGB formation energy at ambient pressure is quite independent of the misorientation within the range $20° < \alpha < 67.4°$. This conclusion is expected to hold, even if the absolute value of GB energies (here about 1.7 J m^{-2}) may depend on the method and approximations used. This type of information is valuable for modelling the mechanical behaviour of polycrystals with coarse-grain methods like finite elements or phase-field modelling.

Variability in grain-boundary structures

Our results show that the atomic structure of grain boundaries changes with pressure. At each target pressure, to find the configuration of the lowest energy, one must probe the energy landscape by translating one grain with respect to the other along the GB. When releasing the pressure, a GB tends to keep its high-pressure atomic structure, because it remains metastable at ambient pressure, as described in Sect. 3.4.

Those metastable configurations can also be obtained by keeping the pressure constant and probing the energy landscape. As an example, Fig. 7 shows γ-surfaces of the {310}[001] grain boundary that we explored with our method at 0 and 30 GPa. At 0 GPa, two metastable states can be distinguished: (a) one containing wide and hollow structural units and (b) one containing compact structural units, with atomic rows inhabiting the GB plane. At 0 GPa, the configuration (a) with hollow structural units is the most stable. When increasing the pressure to 30 GPa, the energy landscape changes, as well as the relative energies of these configurations. Configuration (a) evolves into a configuration (c), which is slightly more compact and remains metastable. The more compact configuration (b) evolves into a very similar configuration (d), and becomes energetically more favourable than configuration (c). To summarize, both configurations are metastable at both pressures, but their relative stabilities are modified by pressure.

The existence of these two configurations means that the compact configuration (b) may form at ambient pressure, depending on the thermodynamic history. Indeed, a similar compact configuration of the {310}[001] GB was observed experimentally at ambient pressure, with high-resolution transmission electron microscopy (HRTEM) by Saito et al.

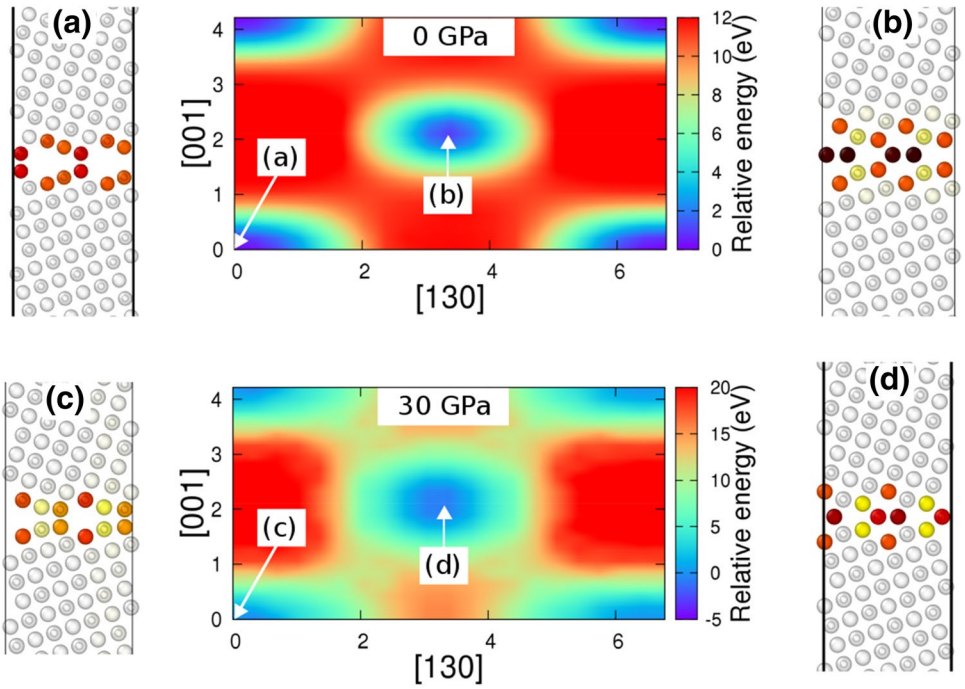

Fig. 7 Evolution with pressure of the γ-surface of the {310} [001] STGB ($\alpha = 36.8°$). The energies relative to the energy of the as-constructed grain boundary ($\boldsymbol{\tau} = 0$) are represented with a colour code, from blue (low energies) to red (high energies), as the top grain is shifted relative to the bottom one by a vector $\boldsymbol{\tau}$ along the GB plane. At 0 GPa, two configurations are metastable: **a** as-constructed symmetric configuration ($\boldsymbol{\tau} = 0$), containing large hollow structural units; **b** more compact configuration, where the top grain was shifted along the GB, and containing atoms inside the plane of the GB. At 30 GPa, both configurations become slightly more compact (**c, d**), and configuration (**d**) becomes more stable than configuration (**c**)

(2013). Another striking example is the {210}[001] STGB, which was observed by HRTEM by Bean et al. (2017). They reported a compact configuration at ambient pressure, corresponding to the one that we computed at 30 GPa (Fig. 3), rather than the hollow one. Bean et al. also performed ab initio calculations on this GB, and acknowledge the fact that the compact configuration is higher in energy than the ground state, but nonetheless, it is the one that formed experimentally in their sample. They explain it by the non-equilibrium growth of the films, and/or by the segregation of vacancies and impurities, that may stabilize the GB into a metastable state instead of the ground state. We would like to stress that the ground-state configurations depicted in the present study are not artefacts from the simulations, because the same configurations are also predicted to be the most favourable ones by more accurate ab initio calculations (McKenna and Shluger 2009; Verma and Karki 2010; Bean et al. 2017). However, because of the out-of-equilibrium thermodynamic history of synthesized or natural samples, the GBs may favour a configuration of low excess volume, rather than the one with the lowest formation enthalpy. These results point to the fact that the atomic structure of a grain boundary does not depend only on the target pressure, but also depends on the pressure history of the sample (and most probably on its temperature history as well), as it was already discussed by Harris et al. (1996) and by Yokoi and Yoshiya (2017).

The structural variability of GBs was recently discussed by Han et al. (2016), who studied STGBs in monoatomic systems (pure Al, Si, and W). These authors argue that in natural or synthesized materials, global thermodynamic equilibrium is seldom reached, and vacancies and impurities tend to segregate at grain boundaries. As a result, GBs are rarely perfectly stoichiometric, and rarely exist in their ground state. In addition to the relative displacement of the grains along the boundary, the authors allowed for an additional degree of freedom by removing atoms inside the GB. By doing so, they found many metastable states, with a wide distribution of formation energies. Natural or synthesized samples are expected to form in one of these metastable states, which may be much more compact than the ground state. It is even possible that the same GB, present in samples with different thermodynamic histories, would exist in different metastable configurations. In the case of an ionic material such as MgO, the removing of atoms raises the problem of charge compensation, as the Mg and oxygen ions are electrically charged. Therefore, we did not include this degree of freedom in our study, but we acknowledge that it should be addressed in future studies.

In fine, one must be very careful when performing numerical simulations of grain boundaries. Limiting the study to one particular configuration (the one of the lowest energy) may not be relevant for practical applications. Several metastable configurations should be considered, including non-stoichiometric configurations in complex materials. The fine atomic structure of GBs is decisive for their electronic properties, their mobility, and many other properties. Such an extensive work remains to be performed in MgO and in other minerals.

Possible implications of the change of STGBs under pressure

Our study demonstrates that under pressures representative of the lower mantle, STGBs exhibit markedly different structures from those observed under ambient conditions. It is thus expected that the contribution of GBs on the physical properties of ferropericlase in the lower mantle cannot simply be inferred from our knowledge of the ceramic MgO at ambient pressure. In what follows, we discuss some possible implications of our calculations on the properties of MgO under high pressure.

Grain growth

The structural changes induced by pressure have a clear influence on the energy cost associated with GBs. Although there is some variability of the formation enthalpy with the precise orientation of the STGB, a clear trend can be observed. Figure 8 summarizes the evolution of STGB formation enthalpies with pressure, taking only high-angle GBs into account. At ambient pressure, the STGB excess energies are well constrained within a narrow range, 1.69 ± 0.07 J m^{-2}. When pressure increases, the GB enthalpies increase to 2.37 ± 0.7 J m^{-2} at 30 GPa, and up to 4.8 ± 0.6 J m^{-2} at 120 GPa. Grain growth is still not well understood, but the driving force of this process is the grain-boundary energy reduction, and in all models, the rate of growth is directly proportional to the GB energy (Burke and Turnbull 1952; Doherty et al. 1997; Humphreys 1997; Evans et al. 2001; Barrales 2008). Assuming parabolic growth kinetics (Burke and Turnbull 1952; Evans et al. 2001), the grain growth rate may increase with pressure, although this increase would be rather modest with a factor of the order of 1.5 between the top and the bottom of the lower mantle. Taking into account the influence of pressure only (thermal activation is also likely to contribute), our calculations on MgO only suggest a small increase of the grain size as a function of depth in the lower mantle. However, a more realistic evaluation of grain growth kinetics would require assessing the mobility of grain boundaries.

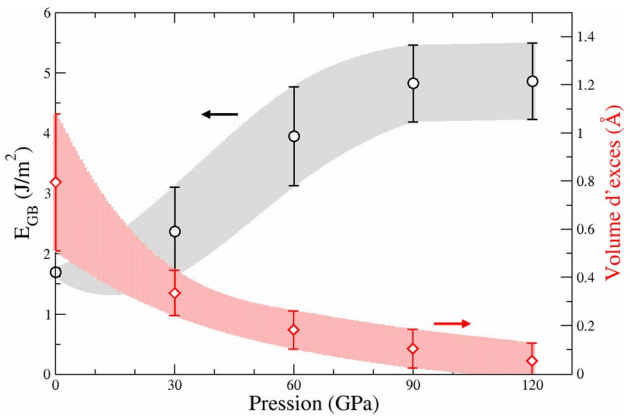

Fig. 8 Evolution with pressure of the average GB formation enthalpy (black circles) and excess volume (red diamonds). The averaging is performed only on high-angle STGBs ($20° < \alpha < 67.4°$). The error bars represent the standard deviation of those values for the high-angle STGBs studied

Impurity segregation

Since the pioneering work of Goldschmidt (Goldschmidt 1937), and the developments of Brice (1975) and Blundy and Wood (1994), it is generally accepted that the problems of trace elements and defect incorporation in solids at a given pressure and temperature are principally controlled by the difference between the ionic radius of the substituent ion and the radius of the host site. According to this model, the size of incorporation sites is the most important parameter controlling ion incorporation and partitioning. Indeed, Blundy and Wood (1994) have shown that the parabolic shape of the experimental plot of partition coefficients as a function of cation radius (the so-called 'Onuma diagram') could be well described by this model based on the physical characteristics (size and elasticity) of the cation sites in the crystal. Recent approaches based on more sophisticated atomistic simulations have confirmed this overall picture (Corgne et al. 2003). The most important virtue of the lattice strain approach is that it allows a fair prediction of partition coefficients even in the absence of experimental data. In its original form, this theory considered only host sites from perfect crystals. Since site size matters, crystal defects which may be associated with free volume (e.g., dislocations and grain boundaries) are likely to play a specific role. In particular, Hiraga et al. (2003, 2004) have shown that impurities tend to segregate preferentially into grain boundaries. Despite the fact that GB sites represent a small fraction relative to the bulk crystal, the significant difference usually observed in sites associated with GB structural units suggests that GBs are likely to store significant amounts of incompatible elements. In MgO which is the focus of the present work, Du et al. (2008) have shown that the solubility of heavier noble gases (one can expect the same behaviour for radiogenic elements) may be considerably enhanced by the presence of interfaces at grain boundaries. More generally, the possibility of large segregation at grain boundaries in MgO has been proposed for several elements including Fe, Si, Ca, or La (Kingery 1979; Chiang et al. 1981; Yan et al. 1998; Wynblatt et al. 2003; Wang et al. 2011; Karki et al. 2015; Feng et al. 2016). Such a strong segregation is likely related to the large, open structural units, which characterize GBs at ambient pressure. Those large vacant

sites offer more space to host foreign atoms than the bulk material.

These considerations can be applied to rocks in the Earth's mantle. Girard et al. (2015) have shown that during shear deformation of a bridgmanite–ferropericlase aggregate, the viscosity contrast between the two minerals leads to layering of (Mg, Fe)O which is likely to lead to increase the fraction of (Mg, Fe)O–(Mg, Fe)O interfaces. However, our results indicate that the dominant effect of pressure, in all STGBs studied, is to close the structural units. Atoms fill in the gaps, and the excess volumes decrease dramatically. Their evolution with pressure is reported in Fig. 8, taking only high-angle STGBs into account. The average excess volume is about 0.8 ± 0.3 Å^3/Å^2 at 0 GPa, and decreases down to 0 to 0.12 Å^3/Å^2 at 120 GPa. Due to this strong steric effect, one can expect the sites at the GBs to become much less attractive for impurities when compared to the situation at ambient pressure. The segregation and binding of impurities at GBs may not be so strong in the extreme conditions of the lower mantle. According to these considerations, GBs may not be the answer to the question of the storage of rare gases and radiogenic elements in the lower mantle. More studies, especially considering interfaces within bridgmanite or between bridgmanite and ferropericlase, are necessary to clarify this issue.

Rheology

Our present study is purely static and does not provide direct information on the dynamic properties of GBs and their contribution to the rheological properties of this phase. Yet, we discuss a few characteristics that are likely to be affected by the pressure-induced structural changes that we report.

Despite the fact that MgO is very refractory, especially under pressure, creep of ferropericlase in the lower mantle occurs in a high-temperature regime, where diffusion likely plays a significant role. Grain boundaries are usually considered as short circuits for diffusion (Osenbach and Stubican 1983; Stubican and Osenbach 1984; Harding and Harris 2001; Karki et al. 2015), again due to the excess volume of the structural units at the interface (as suggested by the anisotropy of accelerated diffusion along the boundary plane). Yet, similar to segregation, the compaction of GB structural units induced by pressure is likely to make migration pathways more intricate and complicated. Indeed, Karki et al. (2015) determined with first-principles calculations that in a {310}[001] STGB in MgO, migration occurs preferentially along the pathways formed by structural units at all pressures from 0 to 100 GPa, making diffusion highly anisotropic. They found that the enthalpy of migration of intrinsic vacancies first decreases when pressure is increased from 0 to 50 GPa, and then increases when reaching 100 GPa. Concerning foreign atoms, they report that migration becomes increasingly difficult as pressure increases. For instance, the activation energy of a Ca ion migrating inside the GB jumps from 0.2 to 1.5 eV when pressure increases from 0 to 50 GPa. Assuming that these results are valid for other GBs, the closing of structural units and drop of excess volume can be expected to severely impede the motion of vacancies and impurities along the grain boundaries. This confining effect due to pressure is likely to inhibit the expected enhanced diffusion along grain boundaries. On the contrary, diffusion at GBs may become very low at high pressure, due to the trapping and limited mobility of point defects.

Finally, there is a growing body of evidence suggesting that GBs are not mechanically inert, but that they can be mobile and produce shear: this is the so-called grain-boundary shear-migration coupling (Cahn et al. 2006). The changes of atomic configurations induced by pressure are expected to result in large variations in the mobility of GBs. In MgO, we show that low-angle STGBs are characterized by GNDs spread in parallel (100) planes at ambient pressure. At high pressure, they decompose into an array of ½<110> dislocations that spread into intersecting {110} planes, a configuration that is known to be much more sessile (Hirth and Lothe 1982). In high-angle STGBs, the change of atomic configuration is also expected to result in large variations of the mobility. The structure of high-angle STGBs is more complex. The notion of GND must be extended to a continuous dislocation density field which must be completed by a continuous disclination field (Sun et al. 2017). Under application of an external stress, these fields are subjected to a force (analogous to the Peach and Koehler force for dislocations) that set GBs in motion and produce shear (Cordier et al. 2012). These fields are intimately related to the GB structure. Hence, structural changes induced by pressure are expected to modify the continuous distribution of defects of the boundary as illustrated on a {310}[001] STGB by Sun et al. (2016). At this point, it remains difficult to assess how these changes affect the mobility of the GB (increase or decrease), but we expect their influence to be significant and this topic clearly requires further attention.

Conclusion

The properties of [001] symmetric tilt grain boundaries in MgO were investigated, using a systematic approach based on atomic-scale calculations. Their formation enthalpy, excess volume, and atomic structure were obtained for pressures ranging from 0 to 120 GPa. At ambient pressure, most STGBs favour a symmetric configuration, and their formation enthalpy is about 1.7 J m^{-2}, quite independent of the misorientation between the two grains. As pressure

increases, most GBs undergo significant structural changes, leading to the closing of structural units to achieve better compaction and to a large drop of excess volumes. Based on elastic model considerations, this is expected to increase grain growth rates when pressure increases and to impede diffusion. Yet, more data from both numerical simulations and experiments will be necessary to properly address these questions and to achieve a better understanding of the rheology of ferropericlase in the Earth's lower mantle.

Acknowledgements We express our warm thanks to two anonymous reviewers, whose questions and comments contributed to greatly improve the clarity and the discussion of the manuscript. This work was supported by funding from the European Research Council under the Seventh Framework Programme (FP7), ERC Grant no. 290424-RheoMan.

References

Amodeo J et al (2011) Multiscale modelling of MgO plasticity. Acta Mater 59:2291–2301. https://doi.org/10.1016/j.actamat.2010.12.020

Appel F et al (1977) Dislocation motion and multiplication at the deformation of MgO single crystals in the high voltage electron microscope. Phys Stat Sol A 42:61–71. https://doi.org/10.1002/pssa.2210420104

Barrales LA (2008) PhD Thesis. RWTH Aachen University

Bean JJ et al (2017) Atomic structure and electronic properties of MgO grain boundaries in magnetoresistive devices. Sci Rep 7:45594

Blundy JD, Wood BJ (1994) Prediction of crystal—melt partition coefficients from elastic moduli. Nature 372:452–454. https://doi.org/10.1038/372452a0

Brice JC (1975) Some thermodynamics aspects of the growth of strained crystals. J Cryst Growth 28:249–253. https://doi.org/10.1016/0022-0248(75)90241-9

Burke JE, Turnbull D (1952) Recrystallization and grain growth. Progress Metal Phys 3:220–244. https://doi.org/10.1016/0502-8205(52)90009-9

Cahn JW et al (2006) Coupling grain boundary motion to shear deformation. Acta Mater 54:4953–4975. https://doi.org/10.1016/j.actamat.2006.08.004

Carrez P et al (2009) Peierls–Nabarro modelling of dislocations in MgO from ambient pressure to 100 GPa. Modell Simul Mater Sci Eng 17:035010. https://doi.org/10.1088/0965-0393/17/3/035010

Carrez, P. et al. (2015): Atomistic simulations of ½ <110> screw dislocation core in magnesium oxide. Comput Mater Sci 103:250–255.

Chiang YM et al (1981) Characterization of grain-boundary segregation in MgO. J Am Ceram Soc 64:385–389. https://doi.org/10.1111/j.1151-2916.1981.tb09875.x

Cordier P et al (2012) Modelling the rheology of MgO under Earth's mantle pressure, temperature and strain rate. Nature 481:177–180. https://doi.org/10.1038/nature10687

Corgne A et al (2003) Atomistic simulations of trace element incorporation into the large site of $MgSiO_3$ and $CaSiO_3$ perovskites. Phys Earth Planet Int 139:113–127. https://doi.org/10.1016/S0031-9201(03)00148-1

Doherty RD et al (1997) Current issues in recrystallization: a review. Mater Sci Eng A 238:219–274. https://doi.org/10.1016/S0921-5093(97)00424-3

Du Z et al (2008) Atomistic simulation of the incorporation of mechanism of noble gaz incorporation in minerals. Geochim Cosmochim Acta 72:554–573. https://doi.org/10.1016/j.gca.2007.10.007

Evans B et al (2001) A few remarks on the kinetics on static grain growth in rocks. Inter J Earth Sci 90:88–103. https://doi.org/10.1007/s005310000150

Eastwood JW et al (1980) P3M3DP—The three-dimensional periodic particle-particle/particle-mesh program. Comput Phys Commun 19:215–261

Feng B et al (2016) Atomically ordered solute segregation behaviour in an oxide grain boundary. Nat Commun 7:11079. https://doi.org/10.1038/ncomms11079

Girard J et al (2015) Shear deformation of bridgmanite and magnesiowüstite aggregates at lower mantle conditions. Science 351:144–147. https://doi.org/10.1126/science.aad3113

Goldschmidt VM (1937) The principles of distribution of chemical elements in minerals and rocks. The Seventh Hugo Müller Lecture, delivered before the Chemical Society on March 17th, 1937

Han J et al (2016) Grain boundary stability and its statistical properties. Acta Mater 104:259–273

Harding JH, Harris DJ (2001) Simulation of grain-boundary diffusion in ceramics by kinetic Monte Carlo. Phys Rev B 63:094102. https://doi.org/10.1103/PhysRevB.63.094102

Harris DJ et al (1996) Atomistic simulation of the effect of temperature and pressure on the [001] symmetric tilt grain boundaries of MgO. Philos Mag A 74:407–418. https://doi.org/10.1080/01418619608242151

Harris DJ et al (1997) Vacancy migration at the {410}/[001] symmetric tilt grain boundary of MgO: an atomistic simulation study. Phys Rev B 56:11477. https://doi.org/10.1103/PhysRevB.56.11477

Harris DJ et al (1999) Computer simulation of pressure-induced structural transitions in MgO [001] tilt grain boundaries. Am Miner 84:138–143. https://doi.org/10.2138/am-1999-1-215

Henkelman G et al (2005) MgO addimer diffusion on MgO(100): a comparison of ab initio and empirical models. Phys Rev B 72:115437

Hiraga T et al (2003) Chemistry of grain boundaries in mantle rocks. Am Miner 88:1015–1019. https://doi.org/10.2138/am-2003-0709

Hiraga T et al (2004) Grain boundaries as reservoirs of incompatible elements in the Earth's mantle. Nature 427:699–703. https://doi.org/10.1038/nature02259

Hirel P (2015) Atomsk: a tool for manipulating and converting atomic data files. Comput Phys Commun 197:212–219. https://doi.org/10.1016/j.cpc.2015.07.012. http://atomsk.univ-lille1.fr

Hirth JP, Lothe J (1982) Theory of dislocations, second edn. McGraw-Hill Publ. Co, New York

Hockney R, Eastwood J (1988) Computer simulation using particles. CRC Press, Boca Raton

Humphreys FJ (1997) A unified theory of recovery, recrystallization and grain growth, based on the stability and growth of cellular microstructures—I. The basic model. Acta Mater 45:4231–4240. https://doi.org/10.1016/S1359-6454(97)00070-0

Karki B et al (2015) First-principles prediction of pressure-enhanced defect segregation and migration at MgO grain boundaries. Am Miner 100:1053–1058. https://doi.org/10.2138/am-2015-5143

Kelchner CL et al (1998) Dislocation nucleation and defect structure during surface indentation. Phys Rev B 58:11085

Kingery WD (1979) Boundary segregation of Ca, Fe, La and Si in magnesium oxide. J Mater Sci 14:1766. https://doi.org/10.1007/BF00569302

McKenna KP, Shluger AL (2009) First-principles calculations of defects near a grain boundary in MgO. Phys Rev B 79:224116. https://doi.org/10.1103/PhysRevB.79.224116

Nzogang B et al (2018) Characterization by scanning precession electron diffraction of an aggregate of bridgmanite and ferropericlase deformed at HP-HT. Geochem Geophys Geosyst 19:582–594. https://doi.org/10.1002/2017GC007244

Osenbach JW, Stubican VS (1983) Grain-boundary diffusion of ^{51}Cr in MgO and Cr-doped MgO. J Am Ceram Soc 66:191–195. https://doi.org/10.1111/j.1151-2916.1983.tb10015.x

Read WT, Shockley W (1950) Dislocation models of crystal grain boundaries. Phys Rev 78:275–289. https://doi.org/10.1103/PhysRev.78.275

Ringwood AE (1991) Phase transformations and their bearing on the constitution and dynamics of the mantle. Geochim Cosmochim Acta 55:2083–2110. https://doi.org/10.1016/0016-7037(91)90090-R

Saito M et al (2013) Local atomic structure of a near-sigma 5 tilt grain boundary in MgO. J Mater Sci 48:5470–5474

Stubican VS, Osenbach JW (1984) Influence of anisotropy and doping on grain boundary diffusion in oxide systems. Solid State Ion 12:375–381. https://doi.org/10.1016/0167-2738(84)90167-X

Stukowski A (2010) Visualization and analysis of atomistic simulation data with OVITO—the open visualization tool. Modell Simul Mater Sci Eng 18:015012. https://doi.org/10.1088/0965-0393/18/1/015012. http://ovito.org

Sun X et al (2016) Influence of pressure on dislocation, disclination, and generalized-disclination structures of a {310}/[001] tilt grain boundary in MgO. J Mater Res 31:3108–3114. https://doi.org/10.1557/jmr.2016.346

Sun X et al (2017) Continuous description of grain boundaries using crystal defect fields: the example of a {310}/[001] tilt boundary in MgO. Eur J Miner 29:155–165. https://doi.org/10.1127/ejm/2017/0029-2609

Tromas C et al (1999) Study of the low stress plasticity in single-crystal MgO by nanoindentation and atomic force microscopy. J Mater Sci 34:5337–5342

Verma AK, Karki BB (2010) First-principles simulations of MgO tilt grain boundary: structure and vacancy formation at high pressure. Am Miner 95:1035–1041. https://doi.org/10.2138/am.2010.3386

Wang Z et al (2011) Atom-resolved imaging of ordered defect superstructures at individual grain boundaries. Nature 479:380–383. https://doi.org/10.1038/nature10593

Watson GW et al (1996) Atomistic simulation of dislocations, surfaces and interfaces in MgO. J Chem Soc Faraday Trans 92:433–438. https://doi.org/10.1039/FT9969200433

Wynblatt P et al (2003) Grain boundary segregation in oxide ceramics. J Eur Ceram Soc 23:2841–2848. https://doi.org/10.1016/S0955-2219(03)00308-X

Yan Y et al (1998) Impurity-induced structural transformation of a MgO grain boundary. Phys Rev Lett 81:3675–3678. https://doi.org/10.1103/PhysRevLett.81.3675

Yokoi T, Yoshiya M (2017) Atomistic simulations of grain boundary transformation under high pressures in MgO. Phys B. https://doi.org/10.1016/j.physb.2017.03.014 **(in press)**